JOURNAL OF MATERIALS SCIENCE **35** (2000) 3089–3096

# Crystallisation kinetics in $AO\text{-}Al_2O_3\text{-}SiO_2\text{-}B_2O_3$ glasses (A = Ba, Ca, Mg)

N. LAHL, K. SINGH, L. SINGHEISER, K. HILPERT
*Institute for Materials and Processing in Energy Systems, Forschungszentrum Jülich GmbH, D-52425 Jülich, Germany*
*E-mail: k.hilpert@fz-juelich.de*

D. BAHADUR
*Department of Metallurgical Engineering and Materials Science, Indian Institute of Technology, Bombay, Mumbai-400076, India*

The crystallisation kinetics of $AO\text{-}Al_2O_3\text{-}SiO_2\text{-}B_2O_3$ glasses (A = Ba, Ca, Mg) was investigated using DTA, XRD, and microstructural studies. Moreover, the influence of nucleating agents such as $TiO_2$, $ZrO_2$, $Cr_2O_3$, and Ni on MgO base glasses was elucidated. The glasses are of interest for the development of sealants in Solid Oxide Fuel Cells (SOFC). The activation energy of crystal growth, $E_a$, was evaluated for the different glasses using the modified Kissinger equation. The preparation method of the glasses seems to determine whether surface or bulk nucleation is the dominant mechanism. The $E_a$ values vary between 330 and 622 kJ/mol. The nucleating agents tend to enhance $E_a$ except $ZrO_2$. An increase of the $Al_2O_3$ concentration induces phase separation and decreases $E_a$. The results are discussed on the basis of the structural role and chemical properties of the Al ions as well as with respect to the possible use of the glasses in SOFC. 

## 1. Introduction

In an effort to develop a suitable sealant for planar solid oxide fuel cells (SOFC), several glass and glass-ceramic systems have been investigated [1–3]. Glasses and glass-ceramics, in principle, meet most of the requirements of an ideal sealant by choosing suitably the components of the glasses and their stoichiometric proportion [1, 4]. Glass ceramics, which can be prepared by controlled crystallisation of glass, possess superior mechanical properties and can have very different thermal expansion coefficients (TEC) due to the different crystalline phases and their volume fraction. To develop a good sealant, it is, therefore, necessary to understand the crystallisation kinetics both from the point of view of their sealing properties and their chemical interactions when in contact with other components of the cell.

With this background, a series of glass sealants of the basic composition, $AO\text{-}SiO_2\text{-}Al_2O_3\text{-}B_2O_3$ (A = Ba, Ca, Mg) was synthesized. Small amounts of $B_2O_3$ were added to reduce the glass transition temperature $T_g$. The content of alumina, an intermediate oxide, has been varied between 5 and 10 mol%. Moreover, additions of nucleating agents such as $TiO_2$, $ZrO_2$, $Cr_2O_3$, and Ni have been tried in MgO base glasses in order to get more insight into the controlled crystallisation process. One of the possible phases formed according to the $MgO\text{-}Al_2O_3\text{-}SiO_2$ phase diagram is cordierite ($Mg_2Al_4Si_5O_{18}$). The cordierite phase, however, is detrimental for the SOFC stack since its thermal expansion coefficient ($2 \times 10^{-6}/^{\circ}C$) is very low compared to other components of the fuel cell. The different nucleating agents were also tried to find out if the crystallisation kinetics can be changed such that the undesirable cordierite phase is suppressed. The crystallisation kinetics of the above mentioned glasses were investigated using differential thermal analysis (DTA), X-ray diffraction (XRD), scanning and transmission electron microscopy (SEM and TEM) with EDX analysis, optical microscopy, and dilatometer measurements. Some of the salient features of these results are presented here.

## 2. Experimental

The glass compositions synthesised and investigated together with their label are given in Table I. The glasses were prepared by taking stoichiometric amounts of different constituent oxides or carbonates, which were then mixed in a ball mill, melted, and quenched. While the glasses 1–8 as well as 12 and 13 (see Table I) were quenched in water, the other glasses were splat quenched between two steel plates to obtain flakes. The chemical analysis of the final products was carried out for each batch using inductive coupled plasma-optical emission spectrometry ICP-OES. The compositions determined are given in Table I. The as prepared glasses were tested by XRD (Philips 1050, Cu $K_\alpha$, as well as STOE, $CoK_{\alpha 1}$) for the amorphous nature of the glass. XRD was also used to find out the crystallisation products of different glasses after heat treatments. The detailed DTA studies were carried out using the thermal analyser (Netzsch STA 429). The glass transition temperature, $T_g$, obtained from DTA was compared with

TABLE I Glass compositions (at %) with label

| Glass | BaO | CaO | MgO | $SiO_2$ | $Al_2O_3$ | $B_2O_3$ | $TiO_2$ | $ZrO_2$ | $Cr_2O_3$ | Ni | Label |
|---|---|---|---|---|---|---|---|---|---|---|---|
| 1 | 45 | | | 45 | 5 | 5 | | | | | BAS |
| 2 | | 45 | | 45 | 5 | 5 | | | | | CAS |
| 3 | | | 45 | 45 | 5 | 5 | | | | | MAS |
| 4 | | | 40 | 45 | 10 | 5 | | | | | MAS10 |
| 5 | | | 38 | 45 | 10 | 5 | 2 | | | | MAST10 |
| 6 | | | 38 | 45 | 10 | 5 | | 2 | | | MASZ10 |
| 7 | | | 43 | 45 | 5 | 5 | 2 | | | | MAST5 |
| 8 | | | 43 | 45 | 5 | 5 | | 2 | | | MASZ5 |
| 9 | | | 35.6 | 43.1 | 12.8 | 3.6 | 4, 9 | | | | MAST12 |
| 10 | | | 43.7 | 44.6 | 6.4 | 3.4 | | | | 1, 9 | MASN6 |
| 11 | | | 46.2 | 42.9 | 6.6 | 3.7 | | | 0, 6 | | MASC6 |
| 12 | | | 33 | 45 | 10 | 5 | 7 | | | | MAS7T10 |
| 13 | | | 38 | 45 | 10 | 5 | | | | 2 | MASN10 |

the softening temperature resulting from dilatometer measurements (Netzsch 402 ED). The dilatometer was further used to obtain the TEC of some typical glasses. Microstructural studies with chemical analysis were carried out using SEM (CAMSCAN) with EDX attachment. The typical glass MAST10 was characterized by the preparation of optical micrographs and by the use of TEM to have insight into the phenomena of phase separation.

## 3. Results and discussion

### 3.1. Glass characterization

The compositions of the samples given in Table I are derived from weighed quantities of the constituents and have been shown to agree with the chemical analyses within 1% to 3%. All the as prepared glasses have been found to be X-ray amorphous exhibiting a broad halo in the X-ray diffraction pattern. The phenomenon of phase separation was studied for one typical glass composition MAST10 by transmission electron microscopy where $TiO_2$ was used as nucleating agent. The TEM studies show a clear evidence of glass in glass phase separation in the nanometer scale. Microprobe analysis with a probe size up to 2 nm was used to obtain some qualitative information about the phase separated region. This analysis suggests that the finely divided macrophase that separated, which has a typical dimension of up to a few nanometers, is slightly richer in $TiO_2$ and $Al_2O_3$ than the matrix. The glasses with $TiO_2$ as nucleating agent are known to have a high tendency for the formation of ordered zones with high $TiO_2$ content due to the high field strength of $Ti^{4+}$ which can cause phase separation and nucleation [5, 6].

### 3.2. Thermal analysis

A typical set of DTA diagrams determined with a heating rate of 10 K per minute and with a particle size of about 15 $\mu$m are shown in Fig. 1 for some of the glasses. Besides the glass transition temperature, $T_g$, all diagrams exhibit one or two exothermic peaks indicating the crystallisation temperatures, $T_c$. All samples show melting above 1100 °C except sample BAS. This sample also exhibits the lowest $T_g$ and $T_c$, as well as more than two exothermic peaks. Moreover, glass BAS shows 100% crystallisation when heated to temperatures $\geq$800°C. Obviously, the crystallisation energy of glass BAS is significantly smaller than that of the other glasses (cf. Fig. 1)

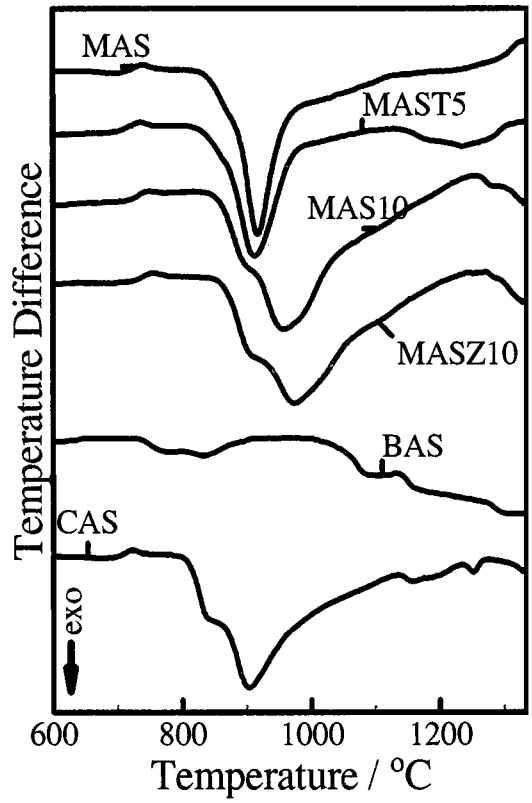


*Figure 1* DTA thermograms determined with a heating rate of 10 K $min^{-1}$ for samples BAS, CAS, MAS, MAS10, MASZ10 and MAST5.

While the samples 1 to 3 in Table I give information on the influence of the alkaline earth metal on the various glass properties, the samples 3 to 13 elucidate the role of nucleating agents as well as the change in concentration of $Al_2O_3$ in $MgO$-$SiO_2$ base glasses. Among the $MgO$-$SiO_2$-$Al_2O_3$ base glasses, those with 5 mol% $Al_2O_3$ exhibit a single exotherm peak while the others with 10 mol% $Al_2O_3$ clearly show two exotherm peaks. The observation of two crystallisation temperatures is an indication of phase separation within the glass, which is supported by TEM studies and some other reports in literature as discussed in the following paragraph.

McDowell and Beall [7] showed that $Al_2O_3$-$SiO_2$ glasses containing less than 5 mol% $Al_2O_3$ do not exhibit any phase separation. However, the glass phase separated with the increase in $Al_2O_3$ content to 10 mol%. The tendency of $Al_2O_3$ to induce phase separation may be explained in terms of the structural role of the $Al^{3+}$ ion [8]. This ion can be four or six coordinated with oxygen giving rise to tetrahedral $AlO_4$ or octahedral $AlO_6$ groups. When it is tetrahedrally coordinated, it takes part as network former. But when the coordination number changes to six, it works as network modifier. For the present magnesium aluminosilicate glasses, it appears that for an $Al_2O_3$ content of 5 mol%, it essentially acts as network former. However, for glasses with 10 mol% $Al_2O_3$, part of it may act as network modifier inducing phase separation.

The crystallisation kinetics of the glasses was investigated by extensive DTA studies using different heating rates and particle sizes. Fig. 2 shows a typical set of DTA diagrams for glasses with small (<10 $\mu$m) and large (10 to 30 $\mu$m) grain size. Table II summarises the important characteristics of DTA results from Figs 1 and 2. The maximum of the exothermal crystallisation peak corresponds to the temperature at which the rate of transformation is maximum. It is interesting to note that the crystallisation peak of the glasses with small particle size is at higher temperature as compared to the glasses with large particle size (samples 1–8 in Table I). There is also a tendency of the splitting of the exothermic peak for these glasses when the large particle size is used. This trend is reverse for the glasses no. 9–13 in Table I. The crystallisation peak of the samples 9–13 with small particle is at a lower temperature than for the large particles which may indicate that the surface nucleation is the dominant mechanism [9–11]. In contrast to this, bulk nucleation seems to be the dominant mechanism for the samples 1–8 in Table I [9–11].

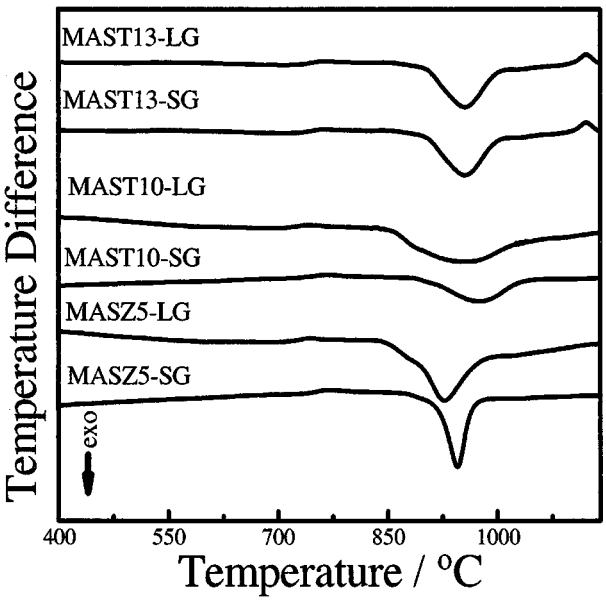


*Figure 2* DTA thermograms of samples (a) MAST10, (b) MASZ5, and (c) MAST13 at a heating rate of 10 K $min^{-1}$ and with two particle sizes of <10 $\mu$m (SG) and >10 $\mu$m (LG), respectively.

The activation energy of crystal growth, $E_a$, was determined by the relationship

$$\ln\left(T^n/T_p^2\right) = -(mE/RT_p) + \text{const} \qquad (1)$$

obtained from the modified Kissinger equation [8]. $T$ is the heating rate, $T_p$ is the peak crystallisation temperature at a given heating rate, $E$ is the apparent activation energy, and $R$ is gas constant. $n$ and $m$ are numerical factors which depend on the crystallisation mechanism.

The factors $n = m = 3$ are taken for bulk nucleation where the crystallisation occurs by the three dimensional growth of crystals. The factors $n = m = 1$ are valid for surface nucleation [8]. The activation energies result on the basis of Equation 1 from the slope of the straight lines shown in Fig. 3 by taking into account the different values of $n$ and $m$ for surface and bulk nucleation. The activation energies obtained are given in Table III. We observe that $E_a$ increases significantly as the alkaline earth metal changes from Ba to Ca and to Mg. These three ions are chemically very different. Their field strength values 0.24 for $Ba^{2+}$, 0.33 for $Ca^{2+}$, and 0.45 for $Mg^{2+}$ [12] change in the same manner. The alkaline earth metals, which act as modifiers, weaken the network and hence ions with lower strength can lead to a higher weakening.

If we compare the $E_a$ values of the different MgO base glasses, the following results are noteworthy:

TABLE II Characteristic transformation temperature $T_g$, crystallisation temperature $T_c$, and peak temperature $T_p$ of the investigated glasses in °C

| Glass | | Large grain | | | | Small grain | | | |
|---|---|---|---|---|---|---|---|---|---|
| | | $T_g$ | $T_{c,1}$ | $T_{c,2}$ | $T_p$ | $T_g$ | $T_{c,1}$ | $T_{c,2}$ | $T_p$ |
| 1 | BAS | 628 | 737 | 810 | 827 | 640 | 744 | 825 | 843 |
| 2 | CAS | 700 | 814 | 846 | 921 | 717 | 826 | 878 | 922 |
| 3 | MAS | 717 | 838 | — | 921 | 731 | — | 900 | 930 |
| 4 | MAS10 | 720 | 860 | 925 | 962 | 736 | 884 | 932 | 972 |
| 5 | MAST10 | 707 | 856 | 890 | 954 | 727 | 886 | 920 | 974 |
| 6 | MASZ10 | 721 | 859 | 938 | 973 | 741 | 890 | 909 | 996 |
| 7 | MAST5 | 712 | 830 | 880 | 913 | 724 | — | 875 | 921 |
| 8 | MASZ5 | 723 | 845 | — | 931 | 740 | — | 894 | 945 |
| 9 | MAST13 | 710 | 858 | — | 955 | 732 | — | 900 | 926 |
| 10 | MASN6 | 735 | — | 892 | 939 | 743 | 855 | 897 | 926 |
| 11 | MASC6 | 738 | — | 897 | 946 | 740 | 870 | 900 | 926 |
| 12 | MAS7T10 | 701 | 871 | 922 | 950 | 715 | 844 | 880 | 926 |
| 13 | MASN10 | 732 | 917 | 960 | 990 | 737 | 880 | 916 | 963 |

TABLE III Activation energy of crystal growth of the different glasses assuming surface nucleation ($n = m = 1$)

| Glass | $E$ (kJ/mol) | Alkaline earth, nucleating agent |
|---|---|---|
| BAS1[a] | 206 | BaO |
| BAS2[a] | 332 | BaO |
| CAS | 413 | CaO |
| MAS | 420 | MgO |
| MAS10 | 343 | MgO |
| MAST10 | 403 | MgO, 2%$TiO_2$ |
| MASZ10 | 311 | MgO, 2%$ZrO_2$ |
| MAST5 | 444 | MgO, 2%$TiO_2$ |
| MASZ5 | 410 | MgO, 2%$ZrO_2$ |
| MASZ13 | 408 | MgO, 4.9%$TiO_2$ |
| MASN6 | 622 | MgO, 1.8%Ni |
| MASC6 | 498 | MgO, 0.6%$Cr_2O_3$ |
| MAS7T10 | 428 | MgO, 7% $TiO_2$ |
| MASN10 | 590 | MgO, 2% Ni |

[a] $E_A$ for two crystallization peaks of sealant BAS.

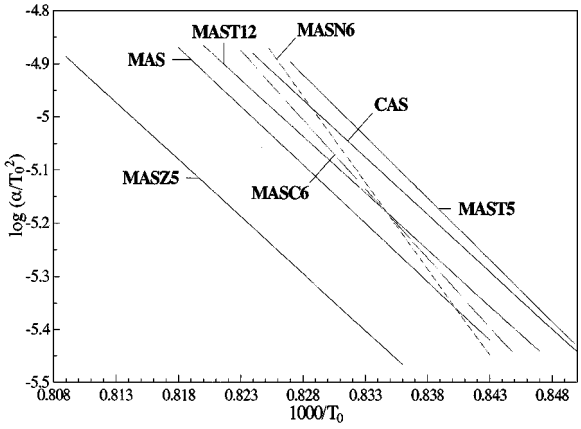


*Figure 3* The modified Kissinger plot of different glass samples.

(1) The $E_a$ values decrease from 451 kJ/mol to about 350 kJ/mol when the $Al_2O_3$ content increases from 5 to 10 mol%.

(2) The $E_a$ values increase if $TiO_2$, $Cr_2O_3$, or Ni are used as nucleating agent. In contrast to this, $E_a$ decreases if $ZrO_2$ is used.

(3) The maximum activation energy of 622 kJ/mol is observed for the sample MASN6 with nickel as nucleating agent. A high value of 498 kJ/mol is obtained for the sample MASC6 with $Cr_2O_3$ as nucleating agent.

As mentioned earlier, $Al_2O_3$ acts as network former if its content is small (up to 5 mol%). However, with the increase of the $Al_2O_3$ content, it acts as network modifier and weakens the network and thus decreases the $E_a$ values. It is interesting to note that all the nucleating agents except $ZrO_2$ tend to enhance $E_a$. Barring $Zr^{4+}$, the other nucleating ions may act as network former, too, as they can have tetrahedral co-ordination besides having a higher co-ordination as modifying ions. The XRD pattern showed also the formation of the $ZrSiO_4$ phase in the $ZrO_2$ containing glasses. In addition to this, Cr in the hexavalent state and the $Ti^{4+}$ ion possess a high field strength imparting a marked ordering effect in these glasses. These may be the reasons for the higher $E_a$ values for the glasses containing $Cr_2O_3$, $TiO_2$, and Ni, as compared to that containing $ZrO_2$ or no nucleating agent.

## 3.3. Phase formation by different heat treatments

In order to have more insight into the crystallisation kinetics, the selected glasses were exposed to two different heat treatments which were selected on the basis of DTA studies. Subsequently, X-ray diffraction and microstructure studies were carried out.

The XRD patterns of the heat treated glasses (annealed at 1000°C for 500 h or 1000 h) show the crystallization of various phases which were identified and are given in Table IV. The percentage of crystallisation was also determined when heated between 800 and 1000°C in the course of different not subsequent heat treatments of the virgin glasses. This is obtained by taking the area under the broad halo and the total area including the one due to crystalline phases. The evaluation was carried out using the software DIFFRAC AT3 supplied by Siemens. Only the glass BAS gets 100% crystallised at all temperatures. The crystallisation of the other glasses amounts between 50% and 90%.

All the glass ceramics show the formation of the $ASiO_3$ phases (A = Ba, Ca, Mg). Most of the Mg containing glasses show additionally the cordierite phase as one of the major products when heated at 1000°C. However, the cordierite phase is less favoured when they are heated below 1000°C. Fig. 4 allows a comparison of the X ray diffraction patterns of glass ceramics obtained by heat treating the glasses MAS5, MAST5, and MASZ5 at 1000°C for 500 h. It is encouraging to note that in glass MAST5, where $TiO_2$ is used as nucleating agent, the cordierite phase is well suppressed. There is also significant difference in the ratio of the clinoenstatite and protoenstatite phases in these three glass ceramics. The XRD patterns of the glasses MAS10, MAST10, and MASZ10, which are given a uniform two stage heat treatment of 750 °C/2 h + 850 °C/23 h, are compared in Fig. 5. The influence of nucleating agents are obvious. The sample MAS10 without nucleating agent exhibits the $MgSiO_3$ (enstatite) phase and a significant amount of glassy phase. A silica rich

TABLE IV Determined phases formed after heat treatment at 1000 °C for 500 h or 1000 h

| Glass | Phases |
|---|---|
| BAS[a] | $BaSiO_3$<br>$BaAl_2Si_2O_8$ |
| CAS[a] | $CaSiO_3$<br>$CaAl_2Si_2O_8$ |
| MAS[a]/MAS10[a]/MAST10[a]/MASC6[a]/ MASN6[b] | $MgSiO_3$<br>$Mg_2Al_4Si_5O_{18}$ |
| MASZ5[a]/MASZ10[a] | $MgSiO_3$<br>$Mg_2Al_4Si_5O_{18}$<br>$ZrSiO_4$ |
| MAST5[a] | $MgSiO_3$<br>$Mg_2Al_4Si_5O_{18}$<br>$Mg_2SiO_4$ |
| MASZ13[b] | $MgSiO_3$<br>$Mg(Al)SiO_3$<br>$Mg_2SiO_4$<br>$TiO_2$ |

[a] Annealing time 1000 h.
[b] Annealing time 500 h.

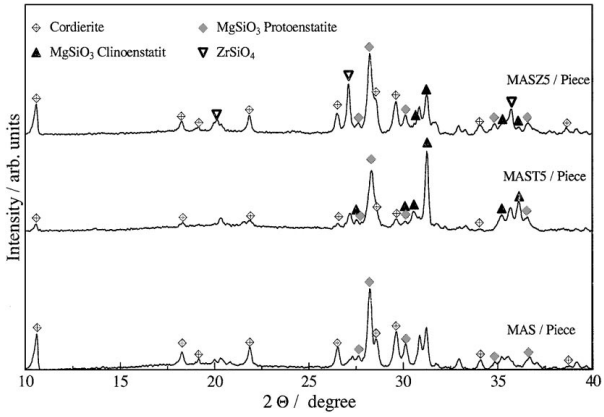


*Figure 4* X-ray diffraction pattern for the glasses (a) MAS, (b) MAST5, and (c) MASZ5 heat treated at 1000°C for 500 h.

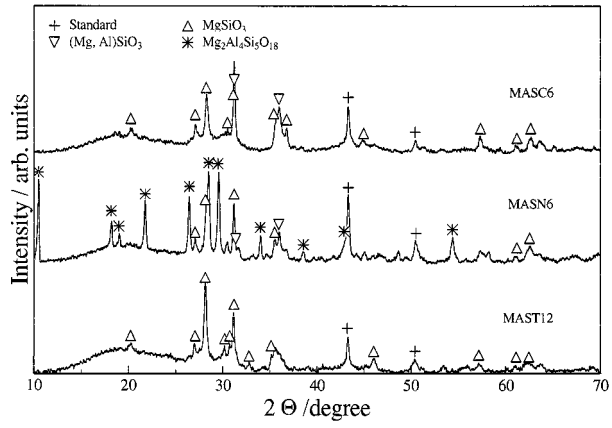


*Figure 6* X-ray diffraction patterns for the glasses (a) MAST13, (b) MASN6, and (c) MASC6 heat treated at 1000°C for 12 h.

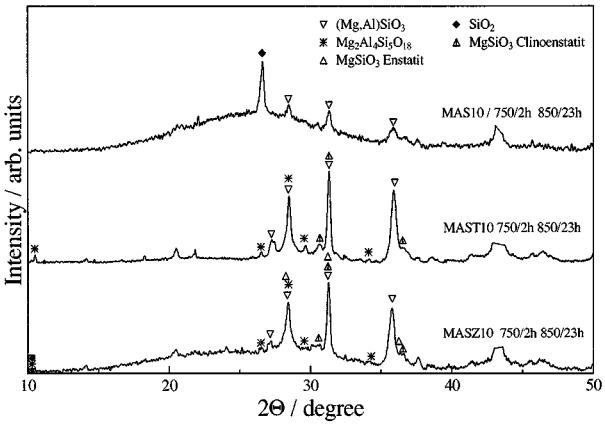


*Figure 5* X-ray diffraction patterns for the glasses (a) MAS10, (b) MAST10, and (c) MASZ10 given a two stage heat treatment of 750 °C/2 h + 850 °C/23 h.

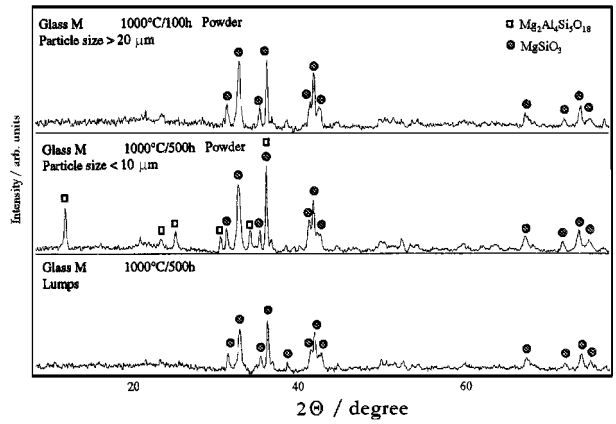


*Figure 7* XRD patterns of glass MASC6 uniformly heat treated at 1000°C for 500 h in (a) bulk form, (b) with average particle size of 20 $\mu$m, and (c) with average particle size of 10 $\mu$m.

phase seems to crystallise in this glassy phase. The same sample shows the formation of the cordierite phase when heat treated at 1000°C over a long time period. Zdaniewski [13] observed similar results and suggests that in the early stages of crystallisation a solid solution rich in $SiO_2$ crystallises. In the later stage, an isomorphic substitution of $Mg^{2+}$ and $Al^{3+}$ occurs, so that the composition approaches that of cordierite. The samples MAST10 and MASZ10 with nucleating agents show more crystallisation and somewhat different crystallisation products as compared to MAS10. They also exhibit a small amount of the cordierite phase. In all compositions investigated, the content of $Al_2O_3$ does not exceed 10 mol%. This fixed $Al_2O_3$ content should in principle limit the formation of the cordierite phase. In contrast to this, the volume fraction of the cordierite phase estimated from the XRD patterns appears to be far larger than what would be expected on the basis of the $Al_2O_3$ content. A careful look at the XRD pattern of some of the glass ceramics (see Fig. 5b) suggests a shift of the XRD lines of cordierite towards lower *d* values indicating a reduction of the lattice parameters. This would mean that the cordierite phase formed is not a pure one. A solid solution is possible if some of the silicon ions occupy $Al^{3+}$ sites. $Si^{4+}$ being smaller than $Al^{3+}$ would then be responsible for the reduction of the lattice parameters. This gets support from EDX point analysis of this glass ceramics, where the Mg : Al : Si ratio of the cordierite deviates from 2 : 2 : 5 and tends to be silica rich. A similar explanation is given by Zdaniewski for the explanation of the crystallisation behaviour of the $SiO_2$-$Al_2O_3$-MgO-$TiO_2$ glass which contains 11 mol% of $Al_2O_3$ [14]. Hence, it appears that a solid solution of the cordierite with the composition $2MgO{\cdot}2Al_2O_3{\cdot}nSiO_2$ may be formed. The value of *n* may depend upon the composition and heat treatment.

The XRD patterns of glass ceramics obtained after annealing the glasses MAST13, MASN6, and MASC6 at 1000°C for 12 h are shown in Fig. 6. The most encouraging result is the complete absence of the cordierite phase in the glass ceramics of MASC6 and MAST13. Both glasses show the same crystallisation behaviour. To investigate it further, the XRD pattern of MASC6 was recorded after a very long heat treatment of 500 h at 1000°C. Bulk material as well as two powders with average grain sizes of 10 $\mu$m and 20 $\mu$m were studied. The XRD patterns of these glass ceramics are shown in Fig. 7. Only the $MgSiO_3$ phase is seen if bulk material was used. No cordierite phase was detected either in the bulk material nor in the particles with a size of larger than 20 $\mu$m. A small fraction of the cordierite phase was detected if the particle size is smaller than 10 $\mu$m. EDX analysis of some of these samples as well as diffusion couples made of the glass and a chromium

base alloy suggest that the chromium ion has an affinity towards the magnesium ion. In such a situation, the magnesium ion besides taking part in the formation of the $MgSiO_3$ phase, gets also coupled to the chromium ion and possibly tends to form a spinel phase which then may suppress the formation of the cordierite phase.

The microstructure of the glass ceramics obtained from the glasses MAS, MAST5, and MASZ5 after a uniform heat treatment at 1000 °C for two 2 h are shown in Fig. 8. These glasses were selected in order to study the influence of the nucleating agents on the crystallisation behaviour. Obviously, there are distinct differences when $TiO_2$ or $ZrO_2$ is used as nucleating agent. Two phases can be distinguished in all three samples besides the matrix phase. A dendritic kind of growth can be seen in the samples with the nucleating agents.

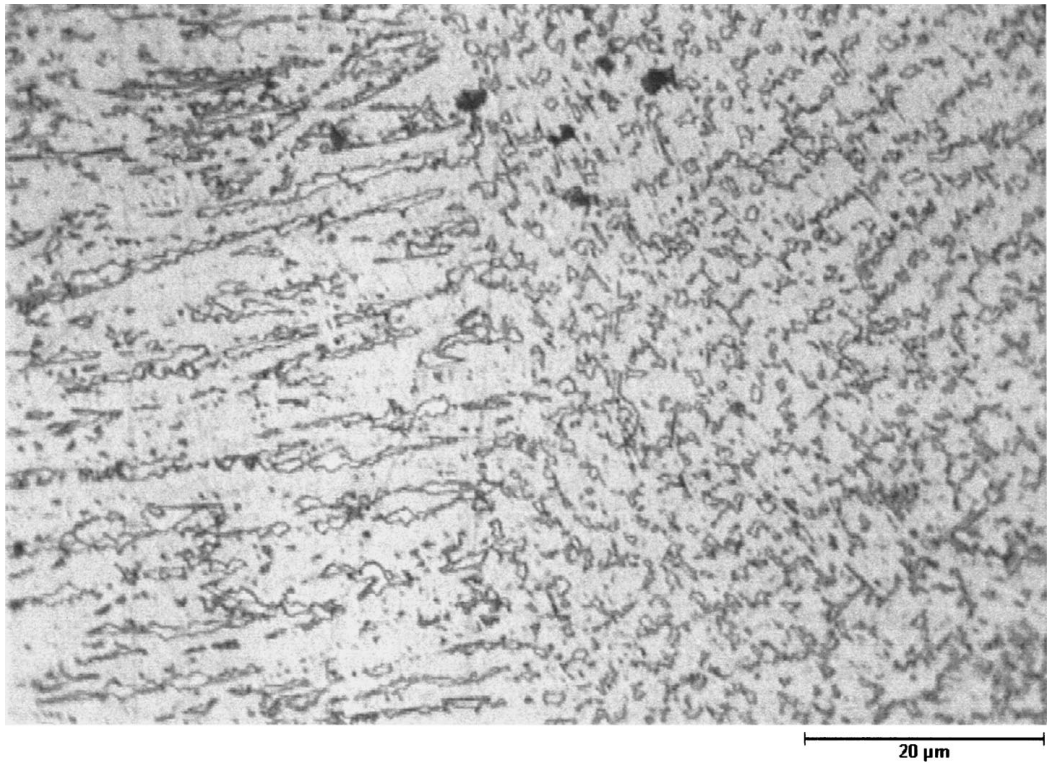


(a)

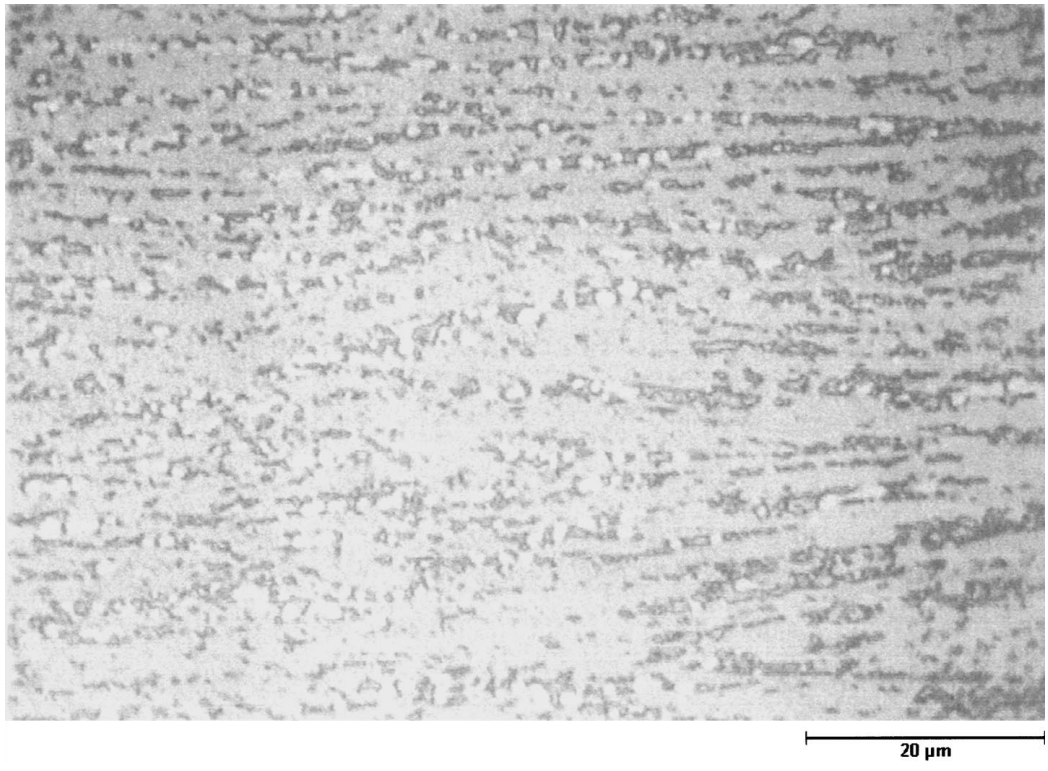


(b)

*Figure 8* Scanning electron micrographs for the glasses (a) MAS, (b) MAST5, and (c) MASZ5 heat treated at 1000°C for 500 h. (*Continued*)

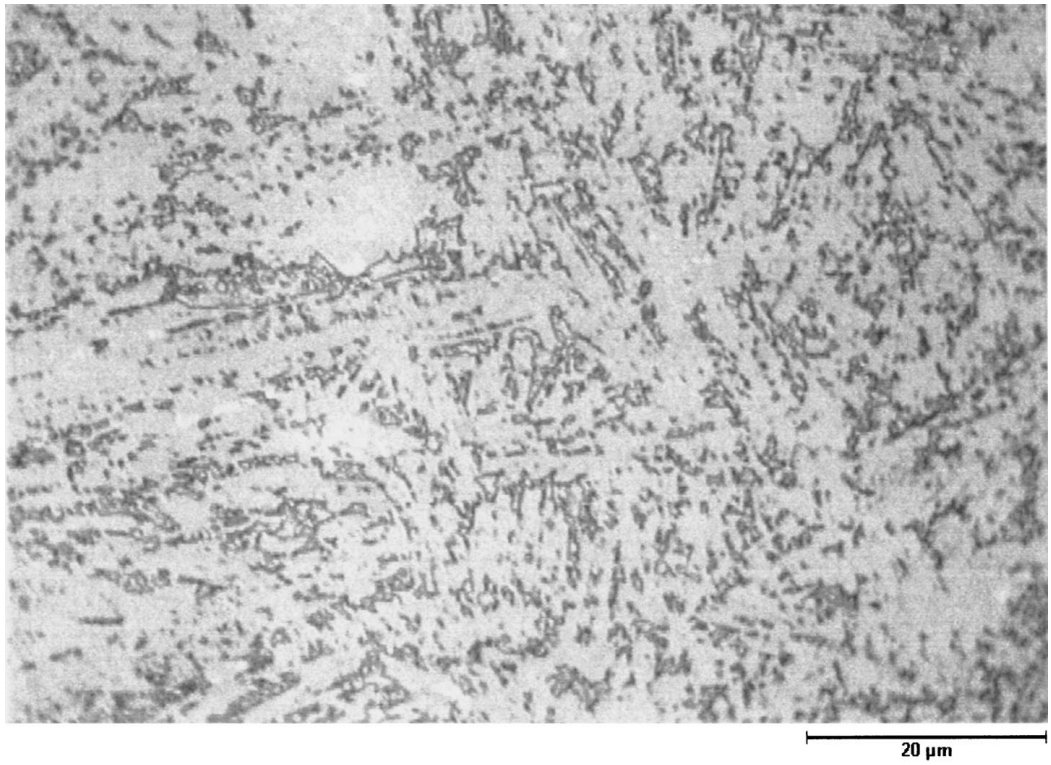


(c)

*Figure 8* (*Continued*).

The sample MAS, without nucleating agent, exhibits a structure which is different from that of the other two samples.

## 3.4. Dilatometer measurements

Dilatometer measurements were carried out on some of the glasses in order to estimate the glass transition temperature and to determine the TEC of the glass ceramics between RT and 1000°C. Glass rods obtained by drawing out of the molten glass and by ceramization (annealing at 1000 °C for 24 h after heating up with 5 K $min^{-1}$ up to 650 °C and with 3 K $min^{-1}$ up to 1000°C) are used in the measurements. The softening temperature from the dilatometer measurements are compared with the $T_g$ values obtained by DTA in Table V. The values obtained by the two different methods agree reasonably well. Thermal expansion data for some selected glasses are given in Fig. 9. The thermal expansion of sealant BAS is the highest which can be explained by the low field strength of the $Ba^{2+}$ ion as compared to those of $Mg^{2+}$ and $Ca^{2+}$ (cf. Section 3.2). Sealant MAS shows a higher thermal expansion than sealant CAS

TABLE V Comparison of the transformation temperature measured by dilatometric measurements and DTA

| Glass | $T_g$/Dilatometer | $T_g$/DTA |
|---|---|---|
| BAS | 608 | 628 |
| CAS | 660 | 700 |
| MAS | 720 | 717 |
| MAS10 | 720 | 720 |
| MAST10 | 708 | 707 |
| MASZ10 | 725 | 721 |

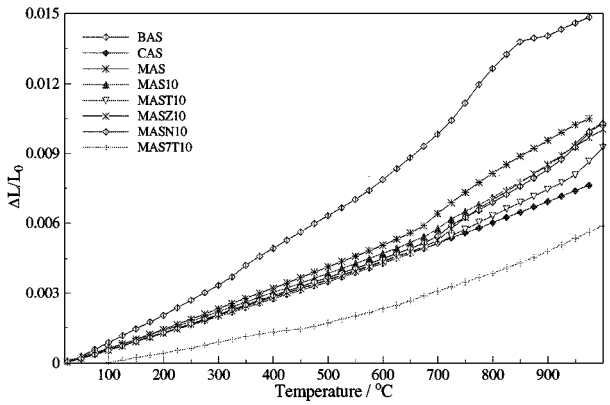


*Figure 9* Plot of thermal expansion for glass ceramics obtained from glasses BAS, CAS, MAS, MAS10, MAST10, and MASZ10 after heat treating the glasses at 1000°C for 24 h.

though the field strength of $Mg^{2+}$ exceeds that of $Ca^{2+}$. This might be caused by the higher degree of crystallisation of sealant CAS as compared to sealant MAS. Most of the MgO containing glass ceramics, particularly those with 10 mol% $Al_2O_3$, show low thermal expansion partly due to significant amounts of cordierite phase in these samples which is known to exhibit a low value of the thermal expansion coefficient. The nucleating agents show practically no influence on the thermal expansion of the sealants MASZ10 and MASN10 unlike for the sealants MAST10 and MAS7T10. The TEC decreased significantly for the latter. The significant decrease for glass MAS7T10 could be explained by the high field strength of $Ti^{4+}$ and the high crystallization degree of the glass rod which became obvious after the crystallisation procedure. The amount of $Ti^{4+}$ in

sealant MAS7T10 is significantly higher than in sealant MAST10 which reduces the TEC.

## 4. Conclusion

The influence of alkaline earth metals A (A = Ba, Ca and Mg), nucleating agents ($TiO_2$, $ZrO_2$, $Cr_2O_3$, and Ni), and $Al_2O_3$ on the crystallization kinetics of AO-$Al_2O_3$-$SiO_2$-$B_2O_3$ glass was investigated. The thermal expansion was additionally considered. The noteworthy conclusions are:

(1) As the alkaline earth metal changes from Ba to Ca to Mg, the activation energy of crystal growth increases significantly which is explained by increasing field strengths. Unlike other glasses, the glass with barium exhibits 100% crystallization when heated to temperatures $\geq 800^{\circ}C$.

(2) If the $Al_2O_3$ content increases from 5 mol% to 10 mol%, it induces phase separation and decreases the activation energy of crystal growth.

(3) The value of the activation energy of crystal growth $E_a$ varies between 330 and 622 KJ/mol. The nucleating agents $Cr_2O_3$ and Ni tend to enhance $E_a$ as they can act as network former too due to their ability to form tetrahedral and higher coordination unlike $ZrO_2$. The high $E_a$ values with Ni and $Cr_2O_3$ as nucleating agents are of interest since they can be used to obtain good wetting behaviour. Besides $MgSiO_3$, cordierite solid solution $2MgO{\cdot}2Al_2O_3{\cdot}nSiO_2$ appears to be another common product in many glasses which is detrimental to SOFC. In this context, the results of glass with $Cr_2O_3$ as the nucleating agent are remarkable, where the cordierite phase is completely suppressed.

(4) BaO as modifier increases the thermal expansion coefficients, TEC, as compared to CaO and MgO. The addition of $TiO_2$ reduces the TEC.


## Acknowledgement

The authors wish to thank Dr. H. J. Penkalla for the TEM investigations. They are also indebted to the International Bureau for the financial support to enable Dr. D. Bahadur to work at Research Centre Jülich. The work was carried out within the JOULE III Programme of the European Community, contract JOE3CT950005.


## References


1. K. L. LEY, M. KRUMPELT, R. KUMAR, J. H. MEISSSER and I. BLOOM, *J. Mater. Res.* **11** (1996) 1489.
2. S. V. PHILLIPS, A. K. DUTTA and L. LAKIN, in Proceedings of the 2nd International Symposium on Solid Oxide Fuel Cells, Athens, July 1991, edited by F. Grosz *et al.* (Commission of the European Communities, Brussels, 1991) p. 737.
3. Y. M. SUNG, *J. Mater. Sci.* **31** (1996) 5421.
4. Z. STRNAD, "Glass Ceramics Materials" (Glass Science & Technology, V8, Elsevier, Amsterdam, 1986).
5. L. BARBIERI, A. B. CORRADI, C. LEONELLI, C. SILIGARDI, T. MANFREDINI and G. C. PELLANI, *Mater. Res. Bull.* **32** (1997) 637.
6. I. W. DONALD, B. L. METCALFE and A. E. P. MORRIS, *J. Mater. Sci.* **27** (1992) 2979.
7. J. F. MAC DOWELL and G. H. BEALL, *J. Amer. Ceram. Soc.* **52** (1969) 17.
8. R. F. DAVIS and J. A. PASK, *ibid.* **55** (1972) 525.
9. C. LEONELLI, T. MANFREDINI, M. PAGANELLI, P. POZZI and G. C. PELLACANI, *ibid.* **26** (1991) 5041.
10. S. H. KNICKERBOCKER, A. H.KUMAR and L. W. HERRON, *Amer. Ceram. Soc. Bull.* **72** (1993) 90.
11. M. J. HYATT and N. P. BANSAL, *J. Mater. Sci.* **31** (1996) 172.
12. A. DIETZEL, *Glastechn. Berichte* **22** Heft 3/4 (1948) 41.
13. W. ZDANIEWSKI, *J. Amer. Ceram. Soc.* **58** (1975) 163.
14. *Idem., J. Mater. Sci.* **8** (1973) 192.



*Received 9 February*
*and accepted 3 December 1999*